

# Cutoff Frequency of Submillimeter Schottky-Barrier Diodes

KEITH S. CHAMPLIN, MEMBER, IEEE, AND GADI EISENSTEIN

**Abstract**—The traditional HF model of a bulk-type (nonepitaxial) Schottky-barrier diode is extended to include the influence of skin effect, carrier inertia, and displacement current. The parasitic cutoff frequency of the extended model is calculated for n-GaAs and n-Si and compared with that predicted by the traditional model. Below the plasma frequency, the two models are found to give similar results for n-Si. For n-GaAs, however, the extended model predicts a value of cutoff frequency only one-sixth that predicted by the traditional model. With both materials, operation *near* the plasma frequency is impractical since it would require unrealistically small contact dimensions. *Above* the plasma frequency, however, both materials display a broad frequency range where operation should again be feasible. For n-Si, the extended model predicts that operation *above* the plasma frequency can actually be achieved with *larger* contacts than is predicted on the basis of the traditional model.

## I. INTRODUCTION

METAL-SEMICONDUCTOR diodes have been used extensively as microwave detectors and mixers since World War II [1]. In recent years, their response has been extended into the submillimeter and far-infrared regions by employing heavily doped, high-mobility semiconductors and by reducing the contact area [2], [3]. Contact radii of the order of  $0.05 \mu\text{m}$  have thus far been achieved [4] by using electron-beam fabrication techniques [5]; and it appears likely that even smaller radii are imminent [6]. At the present writing, mixing at 4.3 THz ( $70 \mu\text{m}$ ) and video detection at 7.1 THz ( $42 \mu\text{m}$ ) using submicron-size bulk-type (nonepitaxial) GaAs diodes have been reported [6], [7].

Van der Ziel has shown theoretically that the fundamental response of the barrier acting alone should extend to frequencies well above the plasma frequency of the bulk material [8]. Recent theoretical work by McColl [6] has considered fundamental limitations on the conversion process imposed by the requisite submicron dimensions. His analysis focuses on the *intrinsic* conversion loss, however, and assumes that high-frequency cutoff due to the inevitably present parasitic elements can be effectively circumvented by making the contact sufficiently small. The purpose of the present paper is to examine the basis for this assumption. Accordingly, it seems currently appropriate to extend the familiar model upon which parasitic cutoff behavior has traditionally been based by including several additional effects of a fundamental nature that can influence submilli-

Manuscript received March 15, 1977, revised May 26, 1977. This work was supported by the National Science Foundation under Grant ENG 75-16587.

The authors are with the Department of Electrical Engineering, University of Minnesota, Minneapolis, MN 55455.

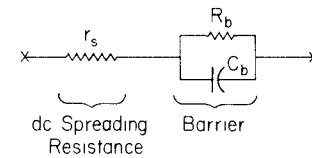


Fig. 1 Traditional model of Schottky-barrier diode. Parasitic cutoff frequency is defined by  $r_s = 1/\omega_c C_b$

meter response. The traditional parasitic model of a bulk-type diode is extended herein to include skin effect, carrier inertia, and displacement current. It is found that for n-type GaAs, and also to a lesser extent for n-type Si, the parasitic cutoff frequency predicted by the extended model differs significantly from that predicted by the traditional model.

## II. THE TRADITIONAL MODEL

The traditional high-frequency model [1, pp. 97–100] of a Schottky-barrier diode consists of the dc spreading resistance  $r_s$  in series with the barrier admittance  $1/R_b + j\omega C_b$  (see Fig. 1). At sufficiently high frequency the barrier capacitance dominates the barrier conductance. Accordingly, a useful “figure-of-merit” has proved to be the frequency at which  $1/\omega C_b$  equals  $r_s$  [9]. This is called the “cutoff frequency” and is written

$$\omega_c = 2\pi f_c = 1/r_s C_b. \quad (1)$$

The dc spreading resistance  $r_s$  results from the constriction of current-flow lines near the contact. For a circular contact of radius  $a$ ,  $r_s$  is given by [1, p. 24]

$$r_s = 1/4a\sigma = 1/4aNq\mu \quad (2)$$

where  $\sigma$  is the semiconductor dc conductivity,  $N$  the carrier concentration, and  $\mu$  the carrier mobility. For a bulk-type diode in which barrier and bulk are formed of like material, the barrier capacitance can be written [1, p. 75 ff]

$$c_b = \frac{(\pi a^2)(q\epsilon N)^{1/2}}{2^{1/2}(\phi_0 - V)^{1/2}} \quad (3)$$

where  $\epsilon$  is the semiconductor permittivity and  $(\phi_0 - V)$  is the height of the barrier as viewed from the semiconductor side. Combining (1)–(3) leads to

$$\omega_c = 2\pi f_c = (4\sqrt{2}/\pi)(\phi_0 - V)^{1/2}q^{1/2}\{N^{1/2}\mu/\epsilon^{1/2}a\} \quad (4)$$

which shows that  $f_c$  varies linearly with the  $(N^{1/2}\mu)$  product and inversely with the contact radius  $a$ .

### III. THE EXTENDED MODEL

One consideration that is lacking in the traditional model is the influence of skin effect on the spreading resistance [10]. At high frequency, the current lines are further constrained to the outer periphery of the contact area. This increases the spreading resistance and causes it to become complex. Dickens [11] has treated this problem and has shown that the high-frequency extension of the spreading resistance is an impedance  $Z$  given by

$$Z = \frac{1}{2\pi\sigma a} \tan^{-1} (b/a) + \frac{(1+j)}{2\pi\sigma d_s} \ln (b/a) \quad (5)$$

where  $b$  and  $a$  are radii of the semiconductor and of the contact, respectively;  $\sigma$  is the semiconductor dc conductivity and

$$d_s = \{2/\omega\mu_0\sigma\}^{1/2} \quad (6)$$

is the classical skin depth in which  $\mu_0$  is the magnetic permeability.

Equation (5) is based on two assumptions that are not generally valid for semiconductors in the submillimeter region. They are

$$\omega \ll \omega_d = (\sigma/\epsilon) \quad (7)$$

where  $\omega_d$  is the "dielectric relaxation frequency," and

$$\omega \ll \omega_s = (q/m^* \mu) \quad (8)$$

where  $\omega_s$  is the "scattering frequency";  $m^*$  being the carrier's effective mass, and  $\mu$  its mobility. Assumption (7) is tantamount to ignoring the displacement current and is the usual skin-depth approximation which leads to (6). Assumption (8) is equivalent to ignoring the mass-inertial behavior of the charge carriers and is not generally justified at high frequency [12].

Both assumptions can be removed from (5) by replacing the dc conductivity  $\sigma$  with the complex quantity<sup>1</sup>

$$\hat{\sigma} + j\omega\epsilon = \sigma \left\{ \frac{1}{1 + j(\omega/\omega_s)} + j(\omega/\omega_d) \right\} \quad (9)$$

and by replacing  $(1+j)/d_s$  with the actual propagation coefficient of the semiconductor material

$$\gamma = \{j\omega\mu_0\}^{1/2} \{ \hat{\sigma} + j\omega\epsilon \}^{1/2} = \frac{(1+j)}{d_s} \left\{ \frac{1}{1 + j(\omega/\omega_s)} + j(\omega/\omega_d) \right\}^{1/2}. \quad (10)$$

Substituting (9) and (10) into (5) and assuming that  $(b/a) \gg 1$  leads to

$$Z = Z_s + Z' \quad (11)$$

where  $Z_s$  is the (complex) bulk-spreading impedance given by

$$Z_s = \frac{1}{4\sigma a} \left\{ \frac{1}{1 + j(\omega/\omega_s)} + j(\omega/\omega_d) \right\}^{-1} \quad (12)$$

<sup>1</sup> Because of lack of detailed information on dielectric dispersion, we will herein assume that  $\epsilon$  is real and equal to its low-frequency value.

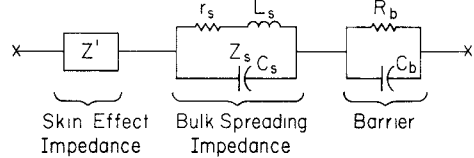


Fig. 2 Extended model of Schottky-barrier diode. Parasitic cutoff frequency is defined by  $\text{Re}\{Z'\} + \text{Re}\{Z_s\} = 1/\omega_c C_b$ .

and where  $Z'$  is the (complex) skin-effect impedance given by

$$Z' = \left\{ \frac{\ln(b/a)}{2\pi} \left| \frac{j\omega\mu_0}{\sigma} \right| \right\}^{1/2} \left| \frac{1}{1 + j(\omega/\omega_s)} + j(\omega/\omega_d) \right|^{-1/2}. \quad (13)$$

An equivalent circuit for the resulting extended model of the Schottky-barrier diode is shown in Fig. 2. One sees that both  $Z'$  and  $Z_s$  appear in series with the barrier admittance. Although the skin-effect term  $Z'$  cannot be represented simply, the bulk-spreading resistance  $Z_s$  can be simply described in terms of three frequency-independent elements [12]. As can be readily shown from (12), they are the dc spreading resistance  $r_s = 1/4\sigma a$ ; the "inertial inductance"  $L_s = r_s/\omega_s$ ; and the "displacement capacitance"  $C_s = 1/r_s \omega_d$ . Parallel resonance of the bulk-spreading impedance  $Z_s$  corresponds to the classical phenomenon of plasma resonance. Thus the classical "plasma frequency" is given by

$$\omega_p = 2\pi f_p = \{L_s C_s\}^{-1/2} = \{\omega_s \omega_d\}^{1/2} \quad (14)$$

and the quality or  $Q$  of this resonance is

$$Q = \omega_p L_s / r_s = \{\omega_d / \omega_s\}^{1/2}. \quad (15)$$

One sees from (14) and (15) that the HF properties of a particular bulk material can be alternatively described in terms of either of two sets of independent parameters. One can choose these parameters to be  $\omega_s$  and  $\omega_d$ ; or alternatively to be  $\omega_p$  and  $Q$ . The former choice is probably the more convenient one when  $\omega_d < \omega_s$ , since the "quality" will then be less than unity and true resonance will not be observed. On the other hand, when  $\omega_s < \omega_d$ , the bulk impedance will actually resonate and the parameters  $\omega_p$  and  $Q$  will most effectively describe this resonance.

### IV. PARASITIC CUTOFF OF THE EXTENDED MODEL

In direct analogy with (1), we define the parasitic cutoff frequency  $\omega_c$  of the extended model by the equation

$$\text{Re}\{Z'(\omega_c)\} + \text{Re}\{Z_s(\omega_c)\} - \frac{1}{\omega_c C_b} = 0. \quad (16)$$

Since both  $Z'$  and  $Z_s$  are reactive, (16) describes a theoretical upper limit to parasitic cutoff that would require a conjugate impedance match in order to be realized.

Consider now the variation of the three terms in (16) with contact radius. According to (13), the first term varies only as  $\ln(b/a)$  and is therefore nearly independent of  $a$ .<sup>2</sup> The

<sup>2</sup> We will assume herein that  $(b/a) \geq 1000$ .

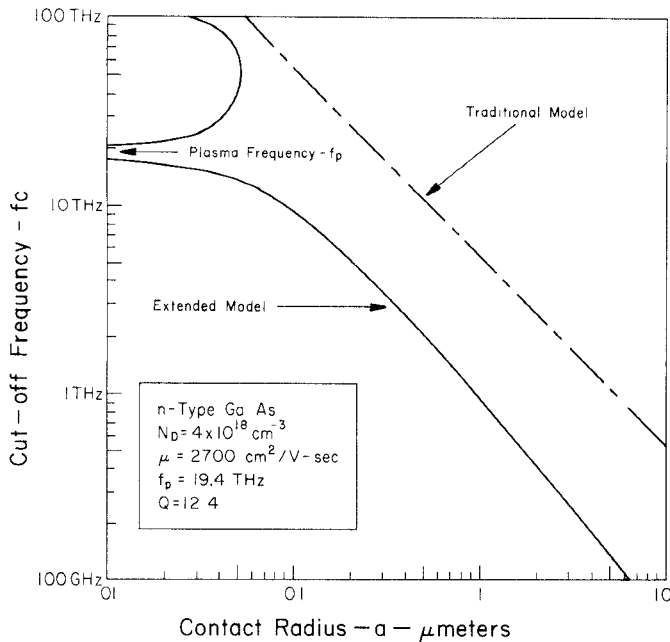


Fig. 3 Parasitic cutoff frequency versus contact radius for n-type GaAs bulk-type Schottky-barrier diode

second term varies as  $(1/a)$  according to (12) and the third term varies as  $(1/a^2)$  according to (3). Thus, for a given material and  $\omega_c$ , (16) can be approximated by a quadratic equation of the form

$$K_0(\omega_c) + K_1(\omega_c)(1/a) - K_2(\omega_c)(1/a)^2 = 0. \quad (17)$$

The solution is written

$$a = \frac{2K_2}{K_1 + \{K_1^2 + 4K_0K_2\}^{1/2}}. \quad (18)$$

Thus, by evaluating  $K_0$ ,  $K_1$ , and  $K_2$  for a given material and cutoff frequency, one can solve (18) to find the appropriate contact radius  $a$ . The results of such calculations are displayed in the next section.

## V. SAMPLE CALCULATIONS

Figs. 3 and 4 show plots of theoretical cutoff frequency as a function of contact radius for diodes fabricated from two different materials and operated at room temperature. The two materials are n-type GaAs and n-type Si, respectively, and the impurity concentrations are intentionally chosen such that the materials have nearly identical plasma frequencies ( $f_p \approx 19$  THz). Note that the plasma  $Q$  of the n-GaAs ( $Q = 12.4$ ) is much larger than that of the n-Si ( $Q = 1.6$ ). This is a direct result of the large difference in mobility between these two materials [13]. For comparison purposes, the parasitic cutoff frequency predicted by the traditional theory (4) is also plotted in Figs. 3 and 4.

## VI. DISCUSSION AND CONCLUSIONS

One sees from Fig. 3 that for n-GaAs, the extended model generally predicts a significantly lower value of  $f_c$  than does the traditional model. Below the plasma frequency, the

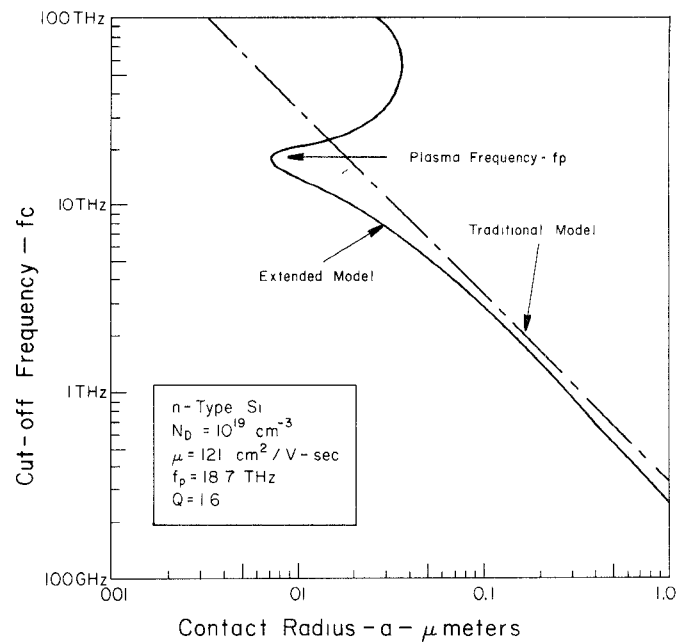


Fig. 4. Parasitic cutoff frequency versus contact radius for n-type Si bulk-type Schottky-barrier diode. (Note change in horizontal scale between Figs. 3 and 4.)

difference is quite pronounced and amounts to approximately a factor of 6. The smaller value of  $f_c$  predicted by the extended model for n-GaAs is undoubtedly due to the skin-effect resistance being large in comparison with the bulk-spreading resistance for this higher conductivity material ( $Z_s$  varies as  $\sigma^{-1}$ , while  $Z'$  varies only as  $\sigma^{-1/2}$ ). One should be aware therefore that the large values of  $f_c$  predicted by the traditional model can probably never be realized with n-GaAs.

With n-Si the situation is quite different. Fig. 4 shows that up to very nearly the plasma frequency, values of  $f_c$  predicted by the two models differ only slightly. Nonetheless, n-GaAs would be the preferred material since a comparison between Figs. 3 and 4 shows that for a given value of radius, the extended model predicts a generally larger value of  $f_c$  for n-GaAs than for n-Si.

Both Figs. 3 and 4 show that operation at, or near, the plasma frequency  $f_p$  is to be avoided since it would require an unrealistically small contact radius. The problem is not as severe with n-Si as with n-GaAs, however, because of the lower  $Q$  of n-Si.

Finally, one sees that there is a fairly broad frequency region centered at about three times the plasma frequency where operation may again be feasible with either material. In this region, carrier inertia (the inductance in Fig. 2) has virtually eliminated the conduction current component so that current flows chiefly as displacement current. Since, according to van der Ziel [8], the barrier itself still responds with at least 25 percent of its low-frequency response at three times the plasma frequency, the region above  $f_p$  may indeed be a fruitful area for future development. For n-Si, the extended model predicts that operation in this region can actually be achieved with *larger* contact dimensions than is predicted on the basis of the traditional model.

## ACKNOWLEDGMENT

The authors wish to thank Professor A. van der Ziel and Dr. U. Lieneweg for many stimulating discussions.

## REFERENCES

- [1] H. C. Torrey and C. A. Whitmer, *Crystal Rectifiers* (Massachusetts Institute of Technology Radiation Laboratory Series, vol. 15). New York: McGraw-Hill, 1948.
- [2] H. R. Fetterman *et al.*, "Submillimeter detection and mixing using Schottky diodes," *Appl. Phys. Lett.*, vol. 24, pp. 70-72, Jan. 15, 1974.
- [3] —, "Submillimeter heterodyne detection and harmonic mixing using Schottky diodes," *IEEE Trans. Microwave Theory Tech.*, vol. MTT-22, pp. 1013-1015, Dec. 1974.
- [4] M. McColl, D. T. Hodges, and W. A. Garber, "Submillimeter-wave detection with submicron size Schottky barrier diodes," in *2nd Int. Conf. Winter School on Submillimeter Waves and their Applications—Conf. Dig.* (Dec. 1976), pp. 62-63.
- [5] M. McColl, W. A. Garber, and M. F. Millea, "Electron beam fabrication of submicrometer diameter mixer diodes for millimeter and submillimeter wavelengths," *Proc. IEEE*, vol. 60, pp. 1446-1447, Nov. 1972.
- [6] M. McColl, "Conversion loss limitations on Schottky-barrier mixers," *IEEE Trans. Microwave Theory Tech.*, vol. MTT-25, pp. 54-59, Jan. 1977.
- [7] D. T. Hodges and M. McColl, "Extension of the Schottky barrier detector to 70  $\mu$ m (4.3 THz) using submicron-dimensional contacts," *Appl. Phys. Lett.*, vol. 30, pp. 5-7, Jan. 1, 1977.
- [8] A. van der Ziel, "Infrared detection and mixing in heavily doped Schottky-barrier diodes," *J. Appl. Phys.*, vol. 47, pp. 2059-2068, May 1976.
- [9] G. C. Messenger and C. T. McCoy, "Theory and operation of crystal diodes as mixers," *Proc. IRE*, vol. 45, pp. 1269-1283, Sept. 1957.
- [10] B. J. Clifton *et al.*, "Materials and processing techniques for the fabrication of high quality millimeter wave diodes," in *Proc. 3rd Biennial Cornell Electrical Engineering Conf.* (Ithaca, NY, 1971), p. 463.
- [11] L. E. Dickens, "Spreading resistance as a function of frequency," *IEEE Trans. Microwave Theory Tech.*, vol. MTT-15, pp. 101-109, Feb. 1967.
- [12] K. S. Champlin, D. B. Armstrong, and P. D. Gunderson, "Charge carrier inertia in semiconductors," *Proc. IRE*, vol. 52, pp. 677-685, June 1964.
- [13] S. M. Sze, *Physics of Semiconductor Devices* New York: Wiley, 1969, p. 40.

# A Wave Approach to the Noise Properties of Linear Microwave Devices

R. P. MEYS

**Abstract**—Noise temperature or noise factor are important parameters for many microwave devices. Their dependence on source characteristics is classically established using low-frequency concepts such as impedance, admittance, voltage, and current sources. This paper presents a derivation of the noise properties of linear two-ports in terms of noise waves, which leads to a convenient measurement method in distributed systems.

## I. INTRODUCTION

THE classical derivations for noise temperature and noise factor of linear two-ports use the equivalent circuit of Fig. 1(a) and lead to the results [1], [2]

$$T_n = T_{n \min} + T_0 \frac{R_n}{G_s} |Y_s - Y_{\text{opt}}|^2 \quad (1)$$

$$F_0 = F_{0 \min} + \frac{R_n}{G_s} |Y_s - Y_{\text{opt}}|^2. \quad (2)$$

Manuscript received March 22, 1977; revised May 27, 1977.  
The author is with the Laboratoire d'Electronique Générale et Radioélectricité, Université Libre de Bruxelles, Brussels, Belgium.

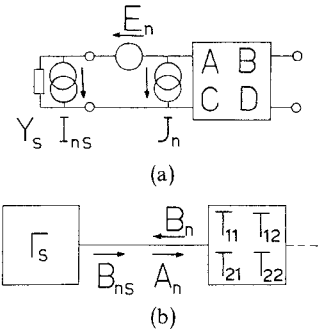


Fig. 1. (a) The classical representation of a linear noisy two-port. (b) The representation of a linear noisy two-port using noise waves.

Sometimes (1) and (2) are written as

$$T_n = T_{n \min} + 4T_0 \frac{R_n}{Z_0} \frac{|\Gamma_s - \Gamma_{\text{opt}}|^2}{|1 + \Gamma_{\text{opt}}|^2(1 - |\Gamma_s|^2)} \quad (3)$$

$$F_0 = F_{0 \min} + 4 \frac{R_n}{Z_0} \frac{|\Gamma_s - \Gamma_{\text{opt}}|^2}{|1 + \Gamma_{\text{opt}}|^2(1 - |\Gamma_s|^2)} \quad (4)$$